COVER SHEET

Title: Design of Composite Double-Slab Radar Absorbing Structures Using Forward, Inverse, and Tandem Neural Networks

Authors: Devin Nielsen
Juhyeong Lee
Young-Woo Nam

(FIRST PAGE OF ARTICLE)

ABSTRACT

The survivability and mission of a military aircraft is often designed with minimum radar cross section (RCS) to ensure its long-term operation and maintainability. To reduce aircraft's RCS, a specially formulated Radar Absorbing Structures (RAS) is primarily applied to its external skins. A Ni-coated glass/epoxy composite is a recent RAS material system designed for decreasing the RCS for the X-band (8.2 – 12.4 GHz), while maintaining efficient and reliable structural performance to function as the skin of an aircraft. Experimentally measured and computationally predicted radar responses (i.e., return loss responses in specific frequency ranges) of multi-layered RASs are expensive and labor-intensive. Solving their inverse problems for optimal RAS design is also challenging due to their complex configuration and physical phenomena.

An artificial neural network (ANN) is a machine learning method that uses existing data from experimental results and validated models (i.e., transfer learning) to predict complex behavior. Training an ANN can be computationally expensive; however, training is a one-time cost. In this work, three different Three ANN models are presented for designing dual slab Ni-coated glass/epoxy composite RASs: (1) the feedforward neural network (FNN) model, (2) the inverse neural network (INN) model – an inverse network, which maintains a parallel structure to the FNN model, and (3) the tandem neural network (TNN) model – an alternative to the INN model which uses a pre-trained FNN in the training process. The FNN model takes the thicknesses of dual slab RASs to predict their returns loss in the X-band range. The INN model solves the inverse problem for the FNN model. The TNN model is established with a pretrained FNN to train an INN that exactly reverses the operation done in the FNN rather than solving the inverse problem independently. These ANN models will assist in reducing the time and cost for designing dual slab (and further extension to multi-layered) RASs.

Devin Nielsen, Department of Mechanical and Aerospace Engineering, Utah State University, Logan, UT 84322.

Juhyeong Lee, Department of Mechanical and Aerospace Engineering, Utah State University, Logan, UT 84322.

Young-Woo Nam, School of Aerospace and Software Engineering, Gyeongsang National University, Jinju, Republic of Korea.

INTRODUCTION

The radar cross section (RCS) of an aircraft is the effective area visible to radar. The survivability and mission effectiveness of military aircraft is often dependent on minimizing its RCS to limit the ranges at which the aircraft can be detected [1]. Radar Absorbing Structures (RASs) are specially-designed materials covering the surface of an aircraft to reduce aircraft's overall RCS, thus increasing its survivability.

In general, RASs are dielectric lossy materials that have low return loss and high directional gain, meaning that they absorb a high fraction of radar microwave and electromagnetic waves rather than reflect them. Conventional RASs are constructed of a high-volume percent of conductive nanoparticles dispersed in an epoxy matrix [2,3]. These RASs have two major disadvantages. *First*, they are difficult to manufacture with a consistent quality because the uniform dispersion of conductive nanoparticles over larger aircraft skins is extremely challenging and requires careful attention to quality in manufacturing and maintenance. The presence of aggregates and non-uniform distribution of conductive particles may locally increase RCS, thus potentially reducing survivability. *Second*, conductive nanoparticle-based RASs typically yield low mechanical strengths [4] and cannot be used as the skin of the aircraft. Therefore, the RAS must be applied on top of the skin of the aircraft. This reduces the fuel efficiency of the aircraft as it must carry the weight of both the RAS and the skin material separately instead of the RAS being the skin of the aircraft [4].

Nam et al. [4–7] have developed thin and lightweight EM wave absorber composites with nickel-plated dielectric fibers via an electroless plating method that provides clues for resolving the problem of nano-conductive particles dispersed in polymer matrix resin. The designed absorber with nickel-plated glass fiber bonded with structural adhesive films was used to achieve their designed thickness, implementing the impedance matching between the developed EM wave absorber and free-space condition. The total thickness of designed nickel-plated absorber with optimization processes used in genetic algorithm for the X-band target has a lightweight and thin thickness compared with conventional absorbers, having excellent absorption performance.

The radar absorbing performance of the Ni-coated glass/epoxy RAS is determined by measuring radar return reflected from a target called a return loss function. Figure 1 shows schematic of geometry of and a representative return loss function for Ni-coated glass/epoxy composites RAS. The return loss is a negative logarithmic value, where a return loss of -10 dB indicates that 99% of the incident radar is absorbed. The return loss function of the dual slab Ni-coated glass fiber RAS is determined by the electric permittivity of the RAS which is dependent on the thicknesses of the slabs [4].

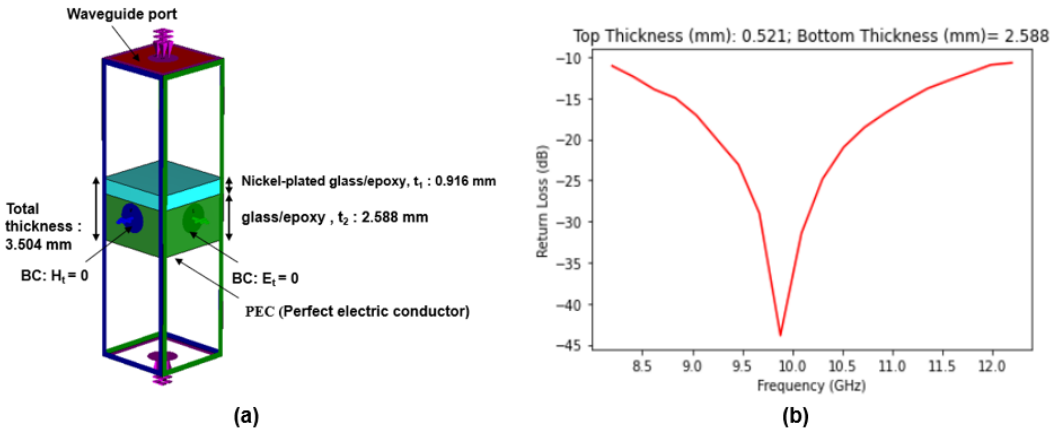

Figure 1. Ni-coated glass/epoxy RAS: (a) electromagnetic simulation model of the double-slab RAS with boundary conditions and (b) representative return loss function.

Experimentally measuring the return loss function of a dual slab Ni-coated glass fiber RAS is labor-intensive (especially for sample preparation) as it requires electroless-plating and lamination of the specimen. It is computationally expensive to simulate the return loss function for dual slab RASs due to complex material configuration and physical phenomena. To ensure sufficient radar absorbing performance, the individuals who design, maintain, and repair aircraft must be capable of predicting the return loss function of a specific RAS and determining what RAS will produce a specific return loss function.

An artificial neural network (ANN) is a machine learning (ML) algorithm that identifies clear relationships between each individual variables and the overall performance of a given dataset. The training process for an ANN is computationally expensive. However, this is a one-time cost. Once the network is optimally trained, the behavior of the system is well characterized and can be used to predict unknown data with high accuracy and low computational costs [8]. Meta material absorbers (MMA) are radar absorbers that combine the effects of polarization conversion and interference cancellation in a single RAS [9]. Chen et al. [9] used a NN-based algorithm to predict the efficiency of MMAs with a constant thickness from the combination of meta-atoms. Ma et al. [10] used a convolutional auto-encoder NN and its inverse network to predict relationship between the geometry of a meta-surface (a two dimensional meta material) and its electromagnetic responses. Hou et al. [11] used a target driven neural network model and its inverse model to determine the relationship between the MMA design parameters and the absorptivity spectrum of the MMAs. The primary focus of this paper is to propose a new methodology for simulating the radar absorbing performance of dual slab Ni-coated glass/epoxy composite RASs using reliable ANN models, which are briefly discussed in the following section.

NEURAL NETWORK

The present work proposes three ANN models developed for the glass/epoxy composite RASs design: (1) the feedforward neural network (*FNN*) model, (2) the inverse neural network (*INN*) model, and (3) the tandem neural network (*TNN*) model. The FNN model (Fig. 2a) predicts the return loss function of the RAS from its top and bottom thicknesses (t_1 and t_2 in Fig. 2). The INN model (Fig. 2b) solves an inverse problem of the FNN model, i.e., t_1 and t_2 are predicted from a specific return loss function. Predicting t_1 and t_2 using an INN model is not straightforward if the training dataset describes a system where multiple RASs could produce the same return loss function (i.e., non-unique case solutions and local minima problems) [8]. The TNN model (Fig. 2c), which can potentially avoid this issue, allows the INN model to converge in spite of non-unique cases in the training dataset [8,12]. In the training process for the TNN model, a trainable INN model is placed in series with a non-trainable, pre-trained FNN model. Therefore, both the input and the output during training is the return loss function of the RAS. As only the INN model is trainable in the TNN, the INN model is trained to exactly reverse the operation done by the FNN model. This leads to the INN model predicting the necessary thicknesses of the RAS, while avoiding the non-unique case problem. Figure 2 summarizes the inputs and outputs of the three ANN models developed in the current study.

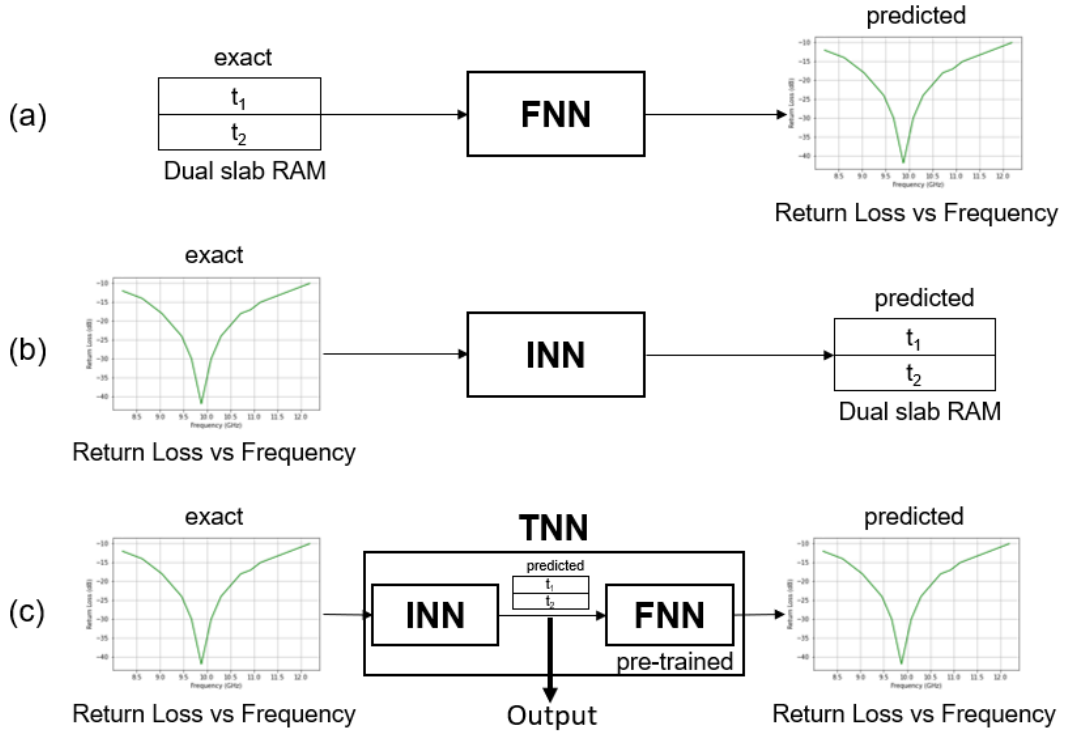

Figure 2. Schematics of neural network models: (a) feedforward neural network (FNN), (b) inverse neural network (INN), and (c) tandem neural network (TNN).

Development

Each ANN model was developed using the Keras API – a python based machine learning software developed as a module of the TensorFlow Library [13]. The experimental dataset of slab thicknesses (t_1 and t_2) and return loss functions, provided by Nam et. al [4], were used to train the models. The RAS specimens (N = 15) had top thicknesses (t_1) ranging from 0.158~1.456 mm and bottom thicknesses (t_2) ranging from 0.412~3.082 mm. These thickness ranges were designated as a baseline in this study. Due to the small size of the experimental dataset (N = 15), the dataset was divided into 90% training and 10% testing in this work. Note that we generated reliable synthetic dataset (N = 1,000~10,000) using the trained FNN model and combined the synthetic dataset with the experimental dataset to develop the INN and TNN models. More details are provided in the following sections.

The FNN models have two input dimensions: top and bottom thicknesses of the dual slab RAS. The return loss function (output of the FNN model) was processed at 20~200 evenly-spaced discrete frequencies to reduce model training time and improve accuracy. As expected, a larger dimensionality (toward 200 frequency data) of model output exponentially increases model training time. Using a small dataset (toward 20 frequency data for each RAS specimen) did not produce a significant increase (< 2%) in model error (i.e., root-mean-square deviation (RMSE), herein). Therefore, the FNN model has an output of 20 return loss values at evenly-spaced frequencies across the X-band. Figure 3 shows the RMSE loss function of each iteration of the training process for the fully developed FNN, INN, and TNN models.

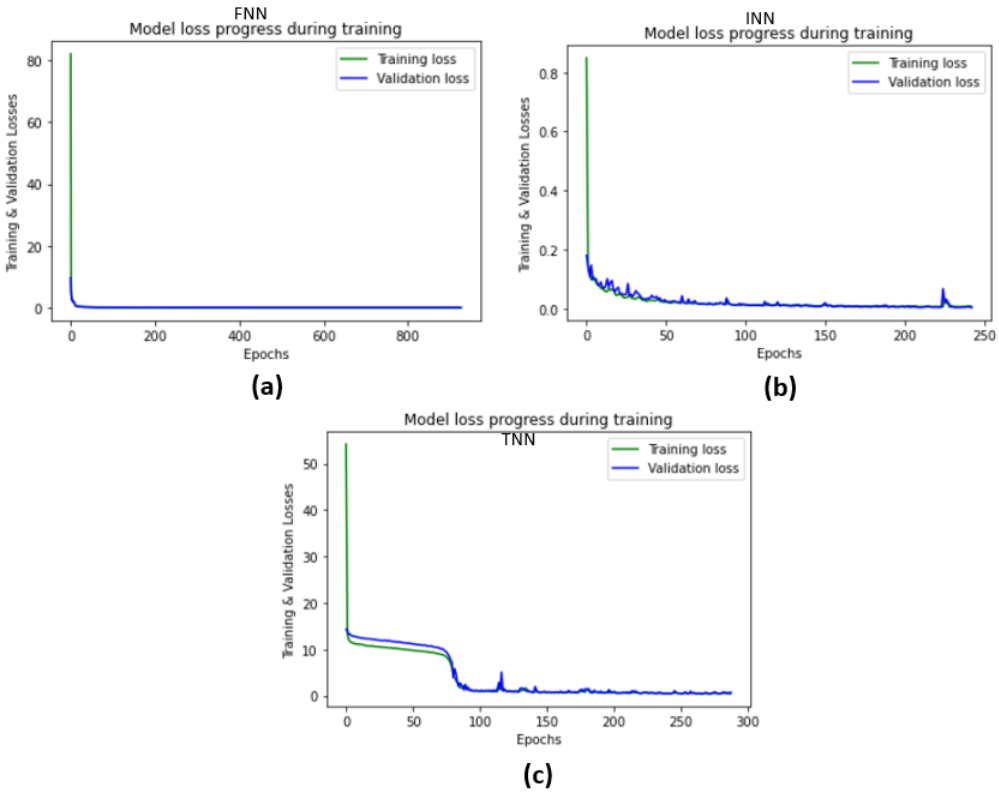

Figure 3. RMSE loss function for: (a) the FNN model trained on an experimental dataset, (b) the INN model trained on a synthetic dataset, and (c) the TNN model trained on a synthetic dataset.

Architecture

A typical NN with a back propagation (BP) algorithm consists of a series of neurons in input, hidden, and output layers. Individual neurons in each layer take the input data, processes it using summation and activation functions, and transfers the results to the neighboring neurons. A BP algorithm iteratively updates the weight (*w*) and bias (*b*) parameters until they reach their optimal values that minimize the variation between a known output and the model's predictions. Figure 4 shows a schematic of a typical FNN architecture with a BP algorithm used for the NNs developed in this study. The INN model has identical architecture, but the inputs and outputs are swapped to solve the inverse problem. As shown in Fig. 2c, the TNN model is constructed based on the INN model and followed by the FNN model.

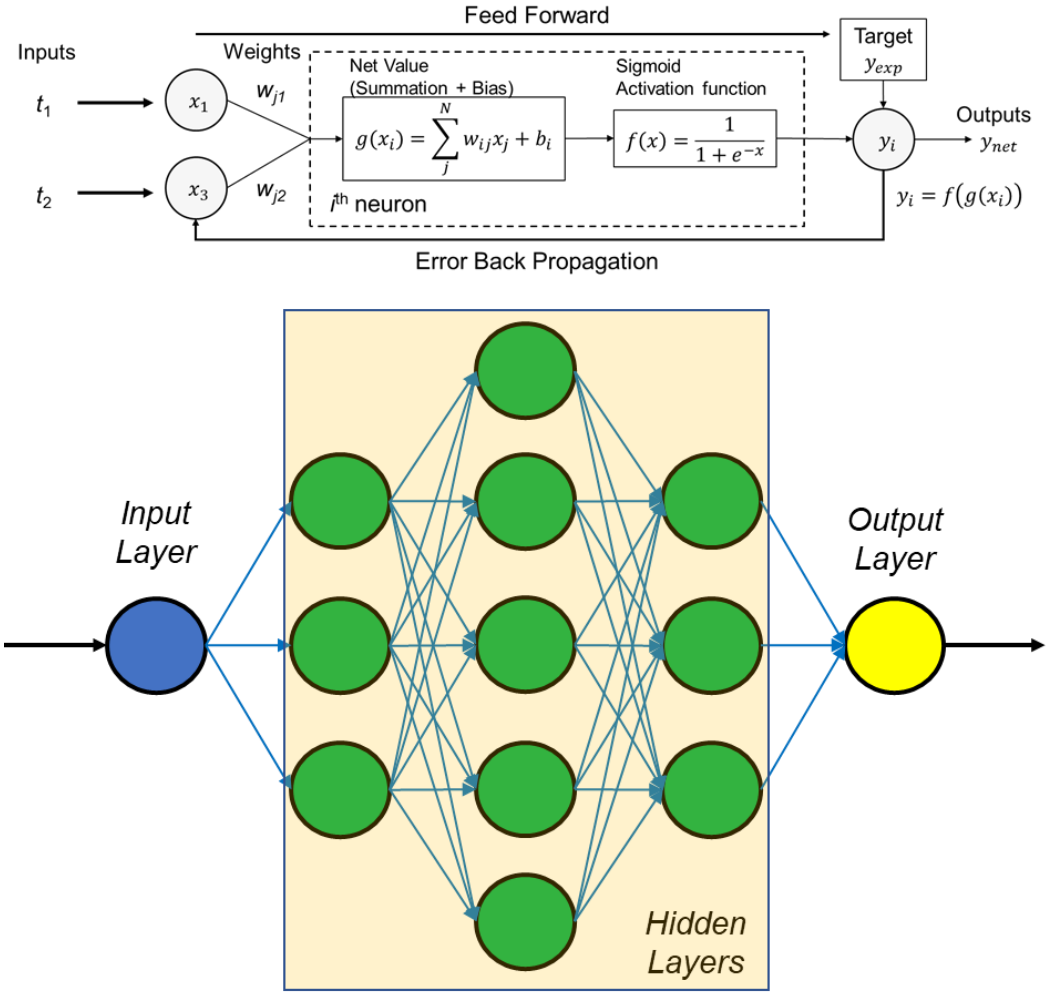

Figure 4. Schematic of FNN architecture with a back propagation algorithm [14].

The total number of neurons and hidden layers are problem-dependent and should be optimization for model accuracy and computational efficiency. In general, an increase in the numbers of neurons and hidden layers are more efficient for solving nonlinear problems but can result in longer computational (training) time, overfitting, and poor predictive performance for simpler problems. Therefore, a preliminary study on hyperparameter optimization (by minimizing RMSE) was conducted for the FNN model. Figure 5 shows the optimized FNN architecture consisting of eight hidden layers, where the number of neurons in each hidden layer varies according to a multiplication factor *m*. In this study, *m* is a user-defined constant that allows the number of neurons in each hidden layer to vary without changing the overall structure of the network. A higher *m* value produces a more accurate neural network, but simultaneously increases training time. Therefore, optimal *m* must be found to provide a *sweet spot* that may exist between model accuracy (i.e., RMSE) and computational efficiency (i.e., training time). Increasing the number of neurons by adjusting the neuron multiplication factor *m* did not significantly decrease the RSME of the FNN model. As shown in Fig. 6, increasing *m* from 2 to 7 decreased the RSME of the FNN model (Fig. 5) by approximately 0.03. This improvement in FNN model performance is not sufficient to compensate for the increased computational costs (i.e., the computational time increases exponentially with *m*). Therefore, the optimal multiplication factor $m = 2$ is used in the following analysis. This indicates that the baseline FNN model constructed 960 neurons in eight hidden layers. The FNN model was developed with Adam optimizer, a learning rate of 10^{-3}, a maximum iteration number of 5000, and early stopping (if the model does not improve after 20 iterations).

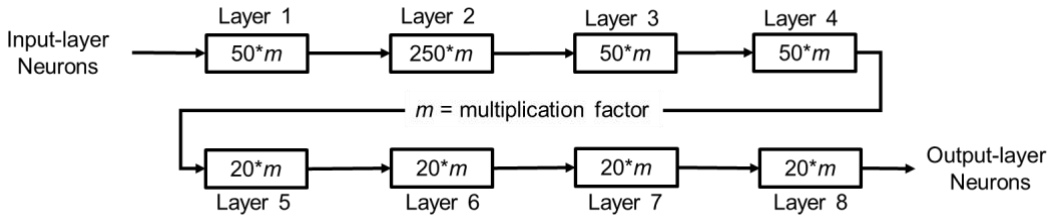

Figure 5. FNN architecture after hyperparameter optimization with multiplication factor *m* determining a number of neurons in each layer.

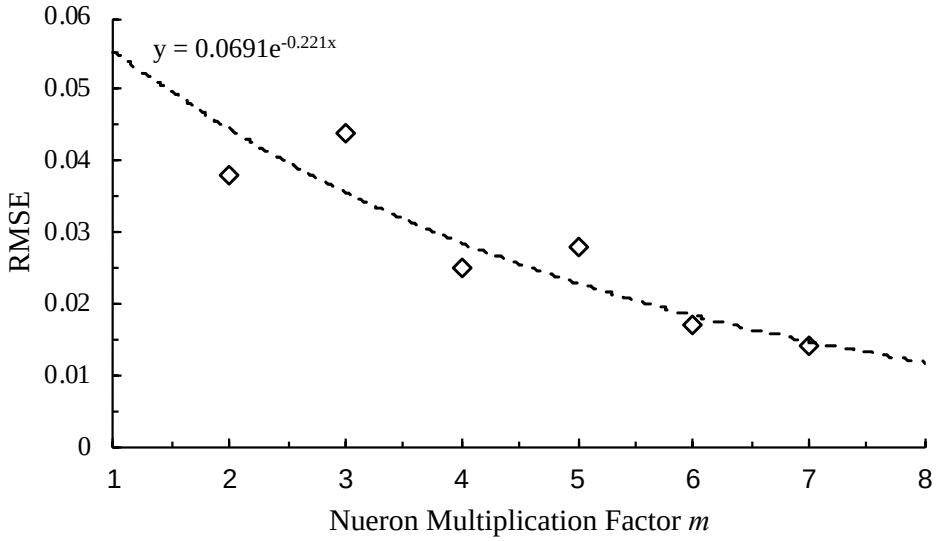

Figure 6. RMSE calculated from the FNN models.

Performance

In the present study, the NN model performance is defined by three metrics: (1) the magnitude of the error function of the network, (2) the slope of the best-fitting line (or linear regression line) and the value of the coefficient of determination (R^2), and (3) the fraction of ill-conditioned return loss functions predicted by the FNN model. *First*, the RMSE metric is used to evaluate the performance of the models developed with experimental dataset only or combined experimental/synthetic dataset. The smaller RMSE refers to better model performance. *Second*, the slope and R^2 value of the linear regression line between the true values and the model predictions are critical parameters in assessing model performance. The slope directly indicates how predicted values are proportional to their actual values, i.e., a slope of 1 means perfect match between true and predicted values. The R^2 is a statistical measure of how close model precision is to the fitted linear regression line. Therefore, the slope measures the accuracy of the model and the R^2 value measures the precision of the model. *Third*, the NN models developed in the current study were initially trained on the limited experimental dataset (N = 15). In this work, the FNN model trained on the small experimental dataset showed superior model performance to the INN and TNN models. Therefore, we generated a large *reliable* synthetic dataset based upon the experimental dataset. The synthetically-generated data may be well-conditioned or ill-conditioned depending on the input data (i.e., t_1 and t_2 for the FNN model). A typical return loss function descends to a global minimum at frequency around 10 GHz before increasing at higher frequencies (Fig. 1 and Fig. 7a). However, ill-conditioned return loss functions (Figs. 7b-7d) from synthetic data generation may have several local minima and unexpected global and local maxima in the X-band. The details on synthetic data generation are discussed in the following section.

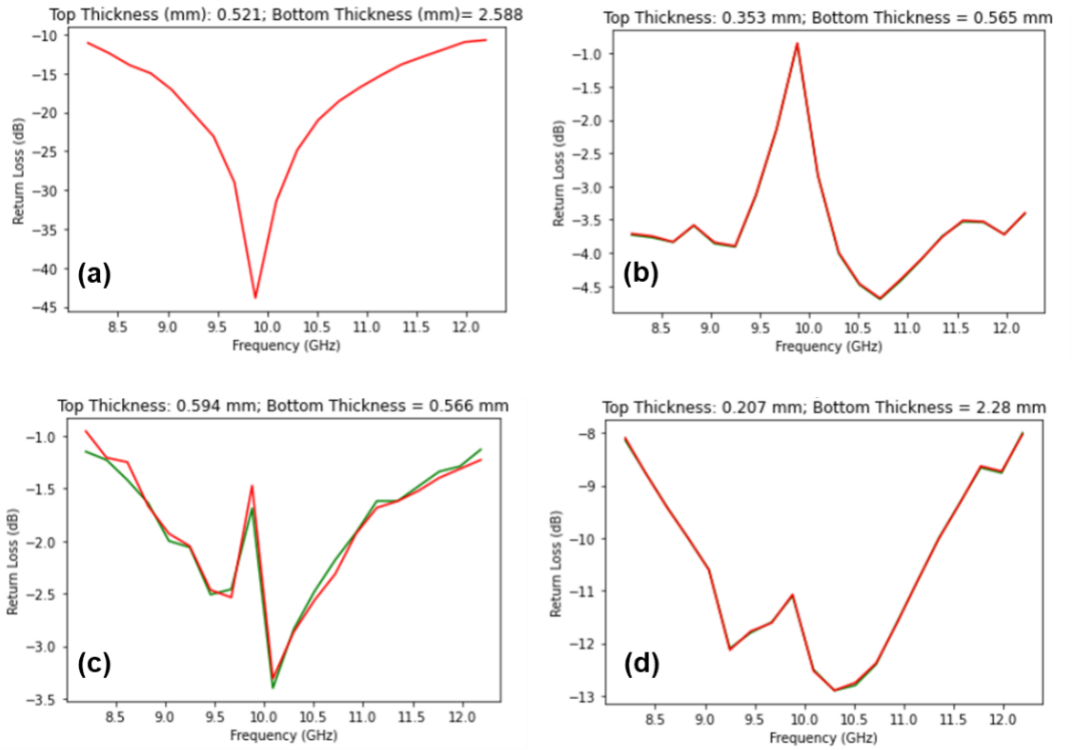

Figure 7. (a) well-conditioned and (b)-(d) ill-conditioned return loss functions. The green and red lines each refers to the synthetically-generated return loss and correspond model prediction.

Synthetic Data Generation

In the FNN model, the relationships between the input (t_1 and t_2) and output (return loss function) variables are relatively straightforward. When trained on an experimental dataset only, the FNN model showed excellent performance in return loss prediction. However, the INN/TNN models trained on an experimental dataset relatively poor predictions due to the complexity of the solution. To overcome such issue and correspondingly improve model accuracy, we generated a synthetic dataset using the pre-trained FNN model using the experimental dataset. The synthetic dataset consisted of three variables (10,000 data points each): t_1, t_2, and return loss. In the synthetic dataset, the t_1, t_2 were generated randomly using a python random number generator function *randint*() within a specified range and the return loss function was predicted from the pre-trained FNN model that takes inputs t_1 and t_2. Figure 8 shows the distributions of synthetic t_1 and t_2 generated using the baseline t_1 (0.158~1.456 mm) and t_2 (0.412~3.082 mm) ranges from the experimental dataset. The range of model input parameters can be adjusted to control ill-conditioned return loss function generation. It is expected that a narrower input parameter range results in less ill-conditioned return loss functions due to the limited size of the experimental dataset.

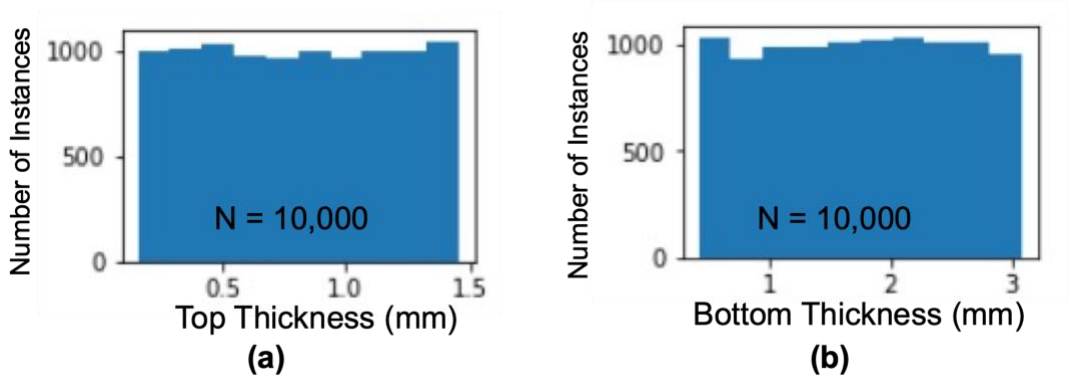

Figure 8. Synthetic data generation: (a) t_1 and (b) t_2.

RESULTS AND DISCUSSION

FNN Model

Figure 9a shows linear curve-fitting between the minimum return loss values captured from an experimental dataset (x-axis) and those predicted from the FNN model (y-axis). Note that the FNN model was trained with only experimental dataset. As shown in the figure, the linear regression plot shows the R^2 value of 0.999, standard deviation σ of 0.011, the slope of 1.005, and the loss function value of 0.081, indicating excellent model performance. Figure 9b compares two representative return loss functions plotted in the X-band frequency range. The FNN model prediction (red line) shows a very good agreement with the experimental observation (green line). The FNN model trained on only experimental dataset provided sufficient accuracy (Fig. 9) and no further training with synthetic data is required. Thus, the FNN model was employed to generate a reliable synthetic dataset to improve the INN and TNN models. Note that a reliable synthetic dataset has relationships between input and out parameters identical to those from an experimental dataset.

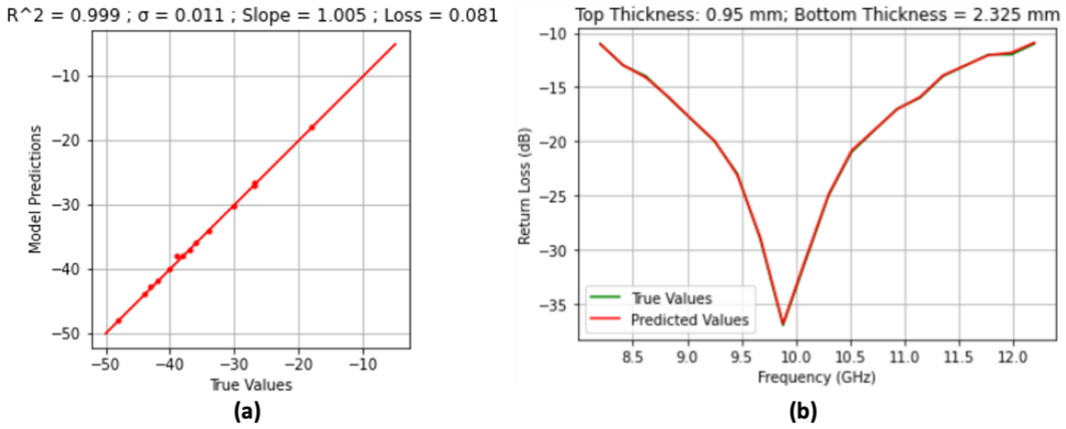

Figure 9. FNN model performance: (a) linear curve fitting between true (experimental) and predicted minimum return loss values and (b) return loss function plotted in the X-band frequency range.

TABLE I. PERCENTAGE OF ILL-CONDITIONED RETURN LOSS FUNCTION PREDICTION FOR VARIOUS T_1 AND T_2 RANGES.

Range	t_1, Top Thicknesses (mm)	t_2, Bottom Thicknesses (mm)	% ill-conditioned return loss function
Baseline	0.158-1.456	0.412-3.082	17.2
1	0.158-1.456	2.186-3.082	2.3
2	0.185-1.456	2.186-3.082	2.1
3	0.259-1.456	2.186-3.082	0.2

The pre-trained FNN model, when taking synthetic t_1 and t_2, may predict ill-conditioned return loss functions. Whenever the top or bottom thickness in the experimental dataset is on the lower end of the thickness range, the other thickness is on the larger end of the thickness range. Therefore, the experimental dataset may not provide sufficient information on the response of dual slab RASs, where both thicknesses are simultaneously on the lower end of the experimental range. Table 1 shows t_1 and t_2 ranges used to generate 1,000 synthetic data points and the percentage of ill-conditioned return loss functions (i.e., Figs. 7b-7d). A decrease in both the t_1 and t_2 ranges reduced ill-conditioned return loss function generation. Furthermore, increasing the lower limit of t_2 from 0.412 to 2.186 mm, while its upper limit remains unchanged, decreased the percentage of ill-conditioned return loss functions from 17.2 to 2.3%. Similarly, increasing the lower limit of t_1 from 0.158 to 0.259 mm also reduced the ill-conditioned return loss functions from 2.3% to 0.2%. Therefore, the FNN models presented in this study predict reasonable results for dual slab RASs with t_1 in the range of 0.259 - 1.456 mm and t_2 in the range of 2.186 - 3.082 mm. The Range 3 in TABLE I was used to generate the 10,000 datapoint synthetic dataset to train the INN and TNN models.

INN Model

Figure 10 compares predicted t_1 and t_2 from the INN models trained on the experimental dataset (N = 15 in Fig. 9a) and the synthetic dataset (N = 10,000 in Fig. 9b). As a reminder, the synthetic datasets is generated using t_1 = 0.259-1.456 mm and t_2 = 2.186-3.082 mm (Range 3 in TABLE I). All statistical parameters (R^2, σ, linear regression slope, and loss function value) indicate that the INN models trained on the synthetic dataset shows excellent model performance and efficiency comparable to the FNN model. In contrast to the limited experimental dataset, the synthetic dataset contains thousands of data points located within the upper and lower limits of t_1 and t_2. As confirmed in Fig. 10, the INN model developed using the synthetic dataset can be a reliable tool for designing dual slab RASs with t_1 and t_2 thicknesses within Range 3.

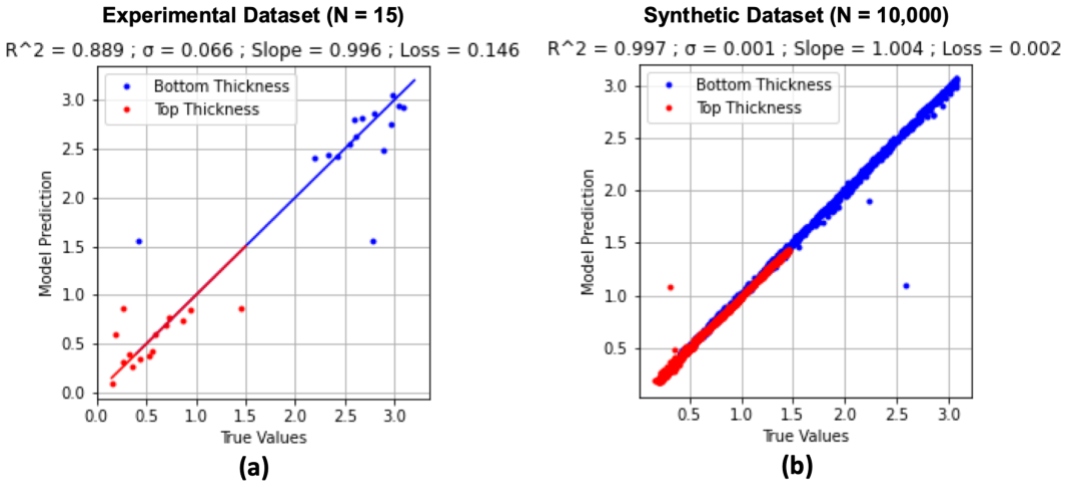

Figure 10. Performance of the INN models trained on (a) experimental and (b) synthetic datasets.

TNN Model

Figure 11 shows linear regression results for the predicted t_1 and t_2 from the TNN models trained on the experimental and synthetic datasets (Fig. 11a and Fig. 11b, respectively). Overall, the TNN model performance was poor compared to the INN models, regardless of dataset size and type. The TNN model improved slightly when trained with the synthetic dataset (Fig. 11), but this was far lower than the FNN model (Fig. 9a) and the INN model (Fig. 10b). Considering only a small improvement of the TNN model performance with N = 10,000 synthetic dataset, the TNN model may achieve an acceptable performance level when N > 1M, making it computationally unfavorable. When an identical synthetic dataset is used for training, the TNN model is less effective than the INN model. This is probably because the relationships between the input and output parameters (t_1, t_2, and return loss function) is simple enough, thus the TNN model may overfit (or have high variance) to the training data, which results in poor testing results in this study. In general, the TNN model likely performs better in predicting more complex relationships defined by larger experimental datasets [8]. TABLE II summarizes the performance parameters of the FNN, INN, and TNN models trained on the experimental and synthetic datasets. The values in the table clearly shows that using a reliable synthetic dataset is beneficial for improving model performance and the INN model performs better than the TNN model for given dataset.

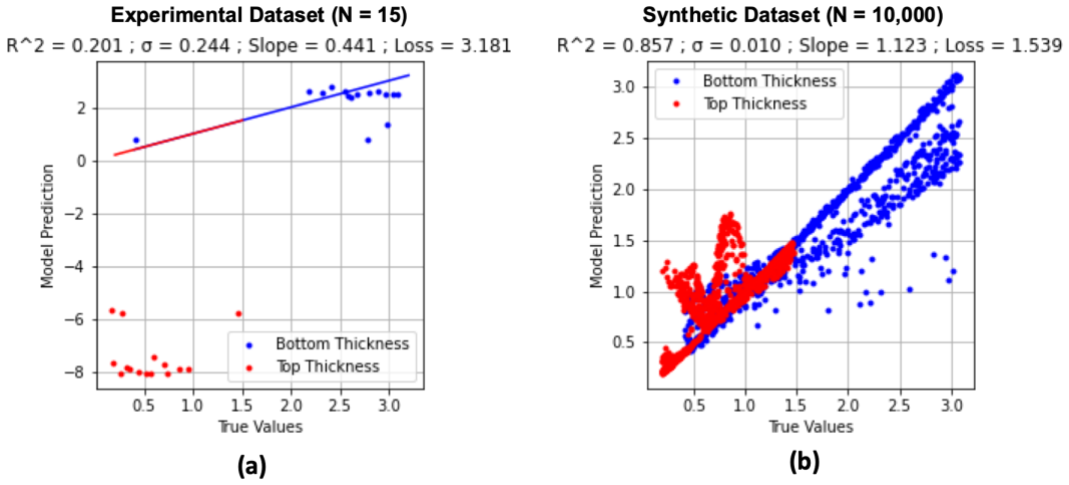

Figure 11. Performance of the TNN models trained on (a) experimental and (b) synthetic datasets.

TABLE II. ANN MODEL PERFORMANCE.

Model	Linear Regression Analysis			
	R^2	Standard Deviation	Slope	RMSE Loss
FNN (Exp.)	0.999	0.011	1.005	0.081
INN (Exp.)	0.889	0.066	0.996	0.146
INN (Syn.)	0.977	0.001	1.004	0.002
TNN (Exp.)	0.201	0.244	0.441	3.181
TNN (Syn.)	0.857	0.010	1.123	1.539

CONCLUSION

This work proposes three artificial neural network (ANN) models developed for the design dual slab Radar Absorbing Structures (RASs): (1) feedforward neural network (FNN), (2) inverse neural network (INN), and (3) tandem neural network (TNN) models. The FNN model takes slab thicknesses to predict RAS's radar responses, while the INN and TNN models are inverse models that predict slab thicknesses from given RAS's radar response. The key findings of the present work are as follows:

- The FNN model after hyperparameter optimization shows excellent performance in return loss prediction, regardless of a dataset's size.
- Using a reliable synthetic dataset generated from an experimental dataset, the performance of the INN and TNN models can be significantly improved.
- The INN model performed better than the TNN model under all conditions, regardless of the experimental and synthetic datasets. The INN model trained on the 10,000 synthetic dataset good model performance compared to the FNN model.

ACKNOWLEDGEMENT

This work was partially supported by the USU Engineering Undergraduate Research Program (EURP).

REFERENCES

[1] Knott, E.F., Shaeffer, J.F. and Tuley, M.T., 1985. "Radar Cross Section: Its Prediction Measurement and Reduction," *Dedham*.

[2] Choi, I. and Lee, D., 2015. "Radar Absorbing Composite Structures Dispersed with Nano-Conductive Particles," *Composite Structures*, *122*, pp.23-30.

[3] Park, K.Y., Han, J.H., Lee, S.B. and Yi, J.W., 2011. "Microwave Absorbing Hybrid Composites Containing Ni–Fe Coated Carbon Nanofibers Prepared by Electroless Plating," *Composites Part A: Applied Science and Manufacturing*, *42*(5), pp.573-578.

[4] Nam, Y.W., Choi, J.H., Lee, W.J. and Kim, C.G., 2017. "Fabrication of a Thin And Lightweight Microwave Absorber Containing Ni-Coated Glass Fibers by Electroless Plating," *Composites Science and Technology*, *145*, pp.165-172.

[5] Nam, Y.W., Choi, J.H., Huh, J.M., Lee, W.J. and Kim, C.G., 2018. "Thin Broadband Microwave Absorber with Conductive and Magnetic Materials Coated on a Glass Fabric," *Journal of Composite Materials*, *52*(10), pp.1413-1420.

[6] Nam, Y.W., Choi, J.H., Lee, W.J. and Kim, C.G., 2017. "Thin and Lightweight Radar-Absorbing Structure Containing Glass Fabric Coated with Silver by Sputtering," *Composite Structures*, *160*, pp.1171-1177.

[7] Nam, Y.W., Choi, J.H., Jang, M.S., Lee, W.J. and Kim, C.G., 2017. "Radar-Absorbing Structure with Nickel-Coated Glass Fabric and Its Application to a Wing Airfoil Model," *Composite Structures*, *180*, pp.507-512.

[8] Liu, D., Tan, Y., Khoram, E. and Yu, Z., 2018. Training deep neural networks for the inverse design of nanophotonic structures. *Acs Photonics*, *5*(4), pp.1365-1369.

[9] Chen, J., Ding, W., Li, X.M., Xi, X., Ye, K.P., Wu, H.B. and Wu, R.X., 2021. "Absorption and Diffusion Enabled Ultrathin Broadband Metamaterial Absorber Designed by Deep Neural Network and PSO," *IEEE Antennas and Wireless Propagation Letters*, *20*(10), pp.1993-1997.

[10] Ma, J., Huang, Y., Pu, M., Xu, D., Luo, J., Guo, Y. and Luo, X., 2020. "Inverse Design of Broadband Metasurface Absorber Based on Convolutional Autoencoder Network and Inverse Design Network," *Journal of Physics D: Applied Physics*, *53*(46), p.464002.

[11] Hou, J., Lin, H., Xu, W., Tian, Y., Wang, Y., Shi, X., Deng, F. and Chen, L., 2020. "Customized Inverse Design of Metamaterial Absorber Based on Target-Driven Deep Learning Method," *IEEE Access*, *8*, pp.211849-211859.

[12] Kabir, H., Wang, Y., Yu, M. and Zhang, Q.J., 2008. "Neural Network Inverse Modeling and Applications to Microwave Filter Design," *IEEE Transactions on Microwave Theory and Techniques*, *56*(4), pp.867-879.

[13] Abadi, M., Agarwal, A., Barham, P., Brevdo, E., Chen, Z., Citro, C., Corrado, G.S., Davis, A., Dean, J., Devin, M. and Ghemawat, S., 2016. "Tensorflow: Large-Scale Machine Learning on Heterogeneous Distributed Systems," *arXiv preprint arXiv:1603.04467*.

[14] Nielsen, D., Lott, T., Dutta, S. and Lee, J., 2021. "Artificial Neural Network (ANN)-Based Predictive Tool for Estimating Lightning Damage in Composites," In the *Proceedings of the American Society for Composites—Thirty-Sixth Technical Conference on Composite Materials*, Sep. 19 – 21, College Station, TX.